Journal of Engineering Physics and Thermophysics, Vol. 83, No. 3, 2010

TRANSONIC FLOW OVER AIRFOILS AT ENERGY INPUT AND WITH ACCOUNT FOR THE REAL PROPERTIES OF THE AIR

S. M. Aul'chenko, V. P. Zamuraev, and A. P. Kalinina

UDC 536.6.011

We have investigated the influence of molecular (thermodynamic and transfer) properties of the air on the qualitative and quantitative characteristics of the gas-dynamic effects of pulsed-periodic energy input in transonic flow over airfoils. The influence of the transfer properties (viscosity) has been taken into account approximately within the boundary layer. It has been shown that qualitative estimates of the above effects do not depend on the account of molecular properties of the air, but the existence of internal degrees of freedom leads to a marked lowering of the temperature level as compared to the ideal gas model. Account of the viscosity somewhat decreases the energy input estimates. The influence of the airfoil shape on the aerodynamic characteristics at energy input has been investigated.

Keywords: *transonic flow, airfoil, molecular properties of air, aerodynamic characteristics, energy input.*

Introduction. At the present time, investigations connected with the active external influence of energy on the flow over bodies in a wide range of flight speeds are being continued [1–6]. The present paper considers transonic regimes of the flow over airfoils. In [3–5], the ideal gas model was used in investigating the effects of pulsed-periodic energy input. However, the energy input proposed in [3–5] leads to a high temperature level (up to a few hundreds of degrees). At these temperatures and low pressures (fractions of atmospheric pressure) excitation of vibrational motion of molecules begins, and their dissociation arises. As a result, the ideal gas model turns out to be unfit.

At the same time, the gas-dynamic effects of energy input obtained in [3] are so interesting that the need arises to investigate them with account for the real properties of the air, both thermodynamic and transfer ones. In [6], the given problem was investigated at continued local heat input with the use of modeling a transonic flow over an airfoil on the basis of Reynolds-averaged Navier–Stokes equations (the specific heat capacities thereby were assumed to be constant). This paper considered various aspects of the effect of energy input on the flow over an airfoil, and an upstream shift of the breakdown shock wave was revealed, which confirms the previously established (see, e.g., [3]) character of the flow restructuring. It should be noted that at the energy source parameters chosen in [6] (position, compact form of the energy source and its power) the lift-drag ratio of the airfoil K did not increase upon feeding energy. On the contrary, in [3–5] the application of pulse-periodic energy sources extending along the airfoil and adjoining it made it possible to obtain a marked increase in the lift-drag ratio upon feeding an energy smaller by two orders of magnitude. In the considered range of Mach numbers of the incident flow, along with the influence of volume energy input, the influence on the resistance of aerodynamic bodies of the heat transfer between the flow and the surface was investigated (see, e.g., [7, 8]).

In the present work we have investigated the influence:

a) of the pulsed-periodic energy input on the gas dynamics of the transonic flow over a symmetric airfoil with account for the thermodynamic properties of the air;

b) of viscosity on the lift-drag ratio of lifting airfoils in the boundary layer approximation at pulsed-periodic energy input;

c) of the shape of airfoils on the control of their lift-drag ratios by means of energy input.

Formulation of the Problem. The flow region is subdivided into an external nonviscous flow and a thin boundary layer. As a mathematical model for describing a plane nonstationary flow of a nonviscous non-heat-conduct-

S. A. Khristianovich Institute of Theoretical and Applied Mechanics, Siberian Branch of the Russian Academy of Sciences, 4/1 Institutskaya Str., Novosibirsk, 630090, Russia; email: aultch@itam.nsc.ru. Translated from Inzhenerno-Fizicheskii Zhurnal, Vol. 83, No. 3, pp. 502–508, May–June, 2010. Original article submitted July 21, 2009.

ing gas, we use the Euler equation in a conservative form with a source term in the energy equation. The system of equations is completed with edge conditions at the boundaries of the doubly connected calculation domain representing a rectangle with an inner boundary corresponding to the considered wing profile contour. On the left, upper, and lower boundaries of this domain, undisturbed flow conditions are set; on the right boundary "soft" conditions are set; and on the wing profile, contour no-flow conditions are set. For the numerical solution of the system of equations, the method described, for example, in [4] is used. In the model under consideration, pulsed energy input is realized instantaneously, with the gas density and velocity remaining unaltered. The energy density of the gas e at the zone of its input increases by the value $\Delta e = \Delta E/\Delta S$. Energy is input in thin zones of approximately rectangular form adjoining the airfoil. For this case, in [3] significant nonlinear effects were obtained. In particular, the numerical experiments of [3] where the period of energy input Δt in the flow is varied over a NACA-0012 airfoil at a Mach number $M_\infty = 0.85$ have shown that the shock-wave structure of the flow strongly depends on the Δt value. At large values of the parameter Δt, for example, at $\Delta t = 0.5$, part of the flow structure is recovered, as a result of which the breakdown shock wave experiences an insignificant upstream shift. In so doing, its position changes within the period. At $\Delta t = 0.05$ the shock wave settles before the energy input zone, and its position remains unchanged within the period. The given value of Δt is considered as a limiting value.

Account of the Real Thermodynamic Properties. To take into account the real thermodynamic properties of the air, two models are used. In the first of them, the air is considered as an ideal mixture O_2–N_2 with constant values of molar concentrations x_m equal to 0.21 and 0.79, respectively. The rotational and vibrational degrees of freedom of molecules are described in the rigid rotator–harmonic oscillator approximation with characteristic vibrational temperatures T_{vm} equal to 2228 and 3336 K for O_2 and N_2, respectively. In this model, the average molar mass of the mixture remains constant and the thermal equation of state of the corresponding equation for the ideal gas $T = \gamma p/\rho$ holds its form, where the temperature T is related to the temperature T_∞ in the incident flow, $\gamma = 1.4$. The specific enthalpy h is calculated from the formula

$$\gamma h = \frac{\gamma T}{\gamma - 1} + \sum_{m=1}^{2} \frac{x_m T_m}{\exp(T_m/T) - 1},$$

where $T_m = T_{vm}/T_\infty$. The specific enthalpy and the internal energy ε are related by the known relation $h = \varepsilon + p/\rho$. The velocity of sound is calculated by the formula

$$a^2 = \left(\left(\frac{\partial \rho}{\partial p} \right)_T - \frac{T}{\rho^2} \frac{\left(\frac{\partial \rho}{\partial T} \right)_p^2}{\left(\frac{\partial h}{\partial T} \right)_p} \right)^{-1}.$$

This model of the thermodynamic properties of the air was used in [9].

In the other model, with account for the real thermodynamic properties of the air, the analytical expressions for the density and specific enthalpy in terms of the pressure and temperature [10]

$$\rho = \rho(p, T), \quad h = h(p, T)$$

are used. These expressions are suitable at temperatures from 200 to 20,000 K and pressures from 0.001 to 1000 atm. The velocity of sound is determined numerically by the above formula.

Comparison of the values of the specific enthalpy, density, and velocity of sound obtained by the formulas of [10] with the known data of the reference book "Tables of Thermodynamic Functions of Air" edited by A. S. Predvoditelev has shown that in the above temperature and pressure ranges the relative deviations for the enthalpy did not exceed 3%, for the pressure they did not exceed 1.5%, and for the velocity of sound the deviations were about 1% up

to temperatures of 10,000 K. The formulas of [10] take into account the vibrational excitation of molecules and their dissociation and single ionization.

The initial distribution of parameters corresponding to the stationary flow over the airfoil without energy input was obtained with an absolute error of 10^{-4} at all mesh points. From the start of energy input to the moment of obtaining a periodic solution, the problem is solved as a nonstationary one. The moment at which the periodic solution reached the steady state was determined by comparing the averaged values of the drag coefficient for the airfoil on time intervals that are multiples of the period of energy input. In so doing, the absolute error did not exceed 10^{-7}.

Boundary Layer. The flow over wings occurs at large Reynolds numbers (of the order of 10^5–10^7). Under such flow conditions, the viscosity has an effect only in a fairly thin layer and, therefore, it can be taken into account from the point of view of the boundary layer model. The choice of the method is based on the known results of G. Yu. Stepanov's work [11]. The approach developed by him for taking into account the viscosity was used successfully by the authors of [12] to solve inverse problems of aerodynamics and by the authors of [13] to solve airfoil design and optimization problems by direct methods. According to [12], the airfoil drag coefficient (without the wave drag component) for a viscous liquid with large Reynolds numbers can be calculated approximately by the following Squire–Young formula:

$$C_{\mathrm{d}} = 2\left(\frac{v_{\mathrm{end}}}{v_\infty}\right)^{3.2} \delta^{**}_{\mathrm{end}}, \quad \delta^{**}_{\mathrm{end}} = \delta^{**}_1 + \delta^{**}_2, \quad \delta^{**}_j = v^n_{\mathrm{end}} \nu^{1/(m+1)} \left[\nu v^{b-2}_{tj} (\mathrm{Re}^{**}_{tj})^a + dA \left| \int\limits_{\Delta_j} |\nu_\tau|^{b-1} \right| d\tau \right]^{1/a},$$

where j = 1, 2; A, b, d, m, n are empirical constants.

The laminar-turbulent transition point of the boundary layer was chosen to correspond to the point of maximum velocity on the upper and lower contours, respectively. In using this approach, two facts should be borne in mind: 1) the calculation of the boundary layer characteristics, if it is fully turbulent, gives overestimated values of losses; 2) all methods for calculating the turbulent boundary layer are based on empirical data pertaining to the incompressible liquid flow $M_\infty = 0$ and the extrapolation of these data to $M_\infty > 0$. Multiple calculations confirmed by experimental data show that at $M_\infty < 1.5$ the boundary layer on single airfoils (and on airfoil lattices) can be calculated with good accuracy, as in an incompressible liquid, if the real (corresponding to the compressible gas flow) velocity distribution is taken. Taking into account the compressibility in calculating the boundary layer leads at the given velocities to a decrease in δ^{**} by a few percent. This is due to the fact that (as the experiment shows) the friction stress weakly depends on the Mach number up to $M_\infty < 1.5$ and the main effect of compressibility on the momentum thickness is produced by the velocity distribution over the airfoil varying with the Mach number of the incident flow.

Results of the Calculations. Calculations with account for the real thermodynamic properties of the air were performed for a NACA-0012 airfoil at a flow over it with a Mach number $M_\infty = 0.85$ at an angle of attack $\alpha = 0$ with a limiting value of the period $\Delta t = 0.05$ (the corresponding dimensionless frequency of energy input $\omega = 20$) and an input energy $\Delta E = 0.001$. The conditions in the incident flow correspond to a flight altitude of 10 km. According to the standard atmosphere tables, $p_\infty = 0.2644$ atm and $T_\infty = 223.15$ K [14]. For one and the same position of the energy input zone ($3.609 \le x \le 3.693$, with the airfoil chord being positioned on a segment $3 \le x \le 4$) calculations by the first gas model gave an insignificant increase in the wave drag coefficient of the airfoil compared to calculations for the ideal gas: instead of $C_x = 0.03498$ a value of $C_x = 0.03507$ was obtained.

At an energy input proportional to the local density of the gas, in the $3.433 \le x \le 3.523$ zone, analogously, instead of $C_x = 0.02156$ for the ideal gas a close (slightly larger) value of $C_x = 0.02162$ for the first gas model was obtained (in this case, the specific input energy $E = 20$ was given, which corresponded to $\Delta E \approx 0.001$).

Thus, account of only the excitation of vibrational molecular motion of the air in calculating its thermodynamic properties in the considered problem has no practical effect on the wave drag of the airfoil as well as on the gas dynamics of the flow over it on the whole.

Calculations with account for the properties of the air by the model of [10] were performed for the first of the variants considered above, i.e., energy $\Delta E = 0.001$ was input in the $3.609 \le x \le 3.693$ zone. In this case, the wave drag coefficient of the airfoil was equal to $C_x = 0.03558$, which was 2% larger than in using the ideal gas model. Account

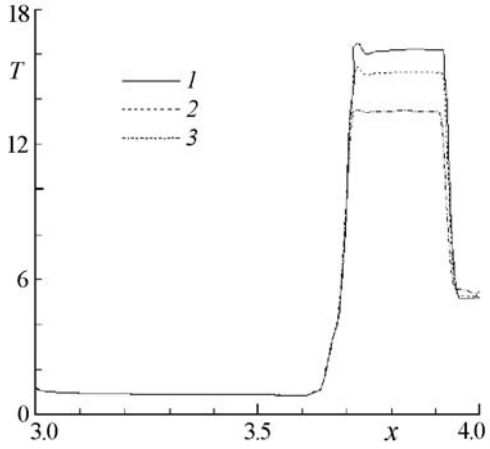

Fig. 1. Temperature distribution along the airfoil: 1) ideal gas model; 2) gas model with account for the excitation of molecular vibration; 3) model of [10].

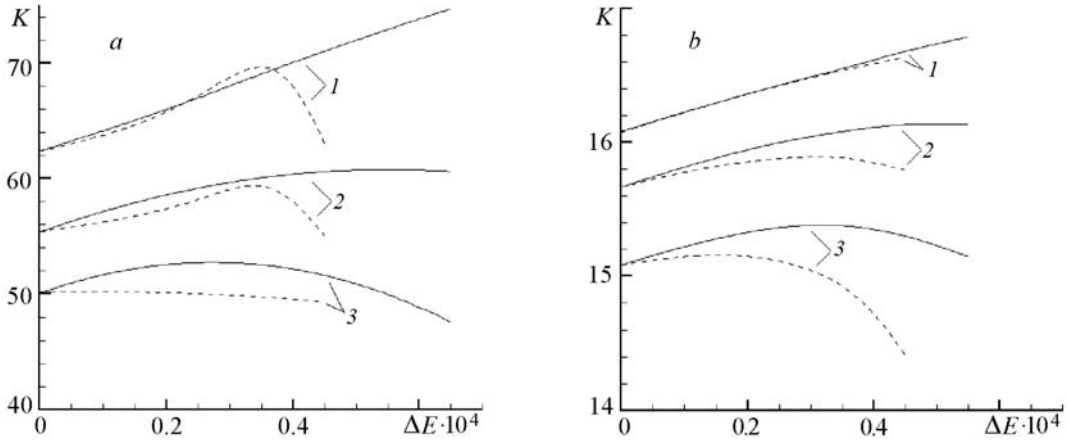

Fig. 2. Lift-drag ratio K of the airfoil versus the input energy for $M_\infty = 0.75$ (a) and $M_\infty = 0.8$ (b) at $C = 12\%$ for various Reynolds numbers: 1) $Re = \infty$; 2) $3 \cdot 10^7$; 3) $3 \cdot 10^6$; solid curves show the energy input zone $3.838 \le x \le 3.864$, dashed curves — $3.567 \le x \le 3.600$.

of the dissociation also slightly affects the wave drag of the airfoil at the considered values of the input energy. This justifies the previous calculations [3–5] with the application of the ideal gas model.

At the same time, account of the real thermodynamic properties of the air leads to a substantial decrease in the airfoil surface temperature after the energy input zone (Fig. 1). Account of only the excitation of vibrational molecule motion leads to a decrease in the temperature by more than 200 deg. Account of the dissociation further decreases the temperature by 500 K. As a result, the air temperature near the airfoil surface does not exceed 3500 deg in the considered variant. In so doing, the position of the breakdown shock wave remains practically unchanged, which leads to a slight change in the wave drag of the airfoil.

The results of calculations with account for the viscosity from the point of view of the boundary layer model are presented in Figs. 2–5. For the variants in Figs. 2–4, the position of the energy input zones $3.567 \le x \le 3.600$ (dashed curves) and $3.838 \le x \le 3.864$ (solid curves) near the downstream face of the airfoil was chosen on the basis of the results obtained by the authors of [5], since the energy input in these zones permits increasing the lift-drag ratio of the airfoil without decreasing the lifting force. Analysis of the results presented was performed for the zone $3.838 \le x \le 3.864$, since in this case the effect is maximum. Figure 2 shows the dependence of the lift-drag ratio K on the input energy for an airfoil of thickness $C = 12\%$ at $M_\infty = 0.75$ (a) and $M_\infty = 0.8$ (b) for various Reynolds numbers. Figure 3 gives the dependence of the lift-drag ratio K on the input energy for an airfoil thickness $C = 8\%$ at

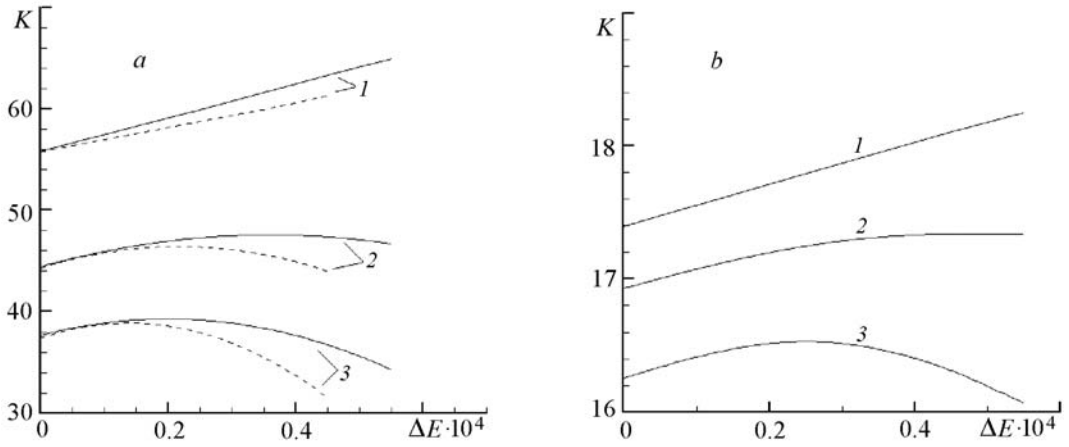

Fig. 3. Lift-drag ratio K of the airfoil versus the input energy for $M_\infty = 0.8$ (a) and $M_\infty = 0.85$ (b) at $C = 8\%$ for various Reynolds numbers. The Re values and designations are same as in Fig. 2.

$M_\infty = 0.8$ (a) and $M_\infty = 0.85$ (b), respectively, for the same Reynolds numbers. Figure 4 shows the dependence of the drag coefficient of the airfoil on the input energy at $M_\infty = 0.8$ and $C = 12\%$.

First of all, the following may be noted: in spite of the increase in the profile drag upon energy input (without the wave drag), in practically all variants energy input permits increasing the lift-drag ratio of the airfoil also with account for the influence of viscosity. The increase in the profile drag is due to the local increase in the pressure in the energy input zone. At the same time, however, there is also a decrease in the value of the wave drag because of the increase in the total pressure in the trailing edge of the airfoil upon energy input, leading to a decrease in the intensity of breakdown shock waves. In so doing, a characteristic feature of the dependence of K on ΔE with account for the viscosity is the presence of a maximum in this dependence. Naturally, the relative increase in the lift-drag ratio with account for the viscosity lessens. For the variant presented in Fig. 2a, the maximum increase in K is 10% for $\mathrm{Re} = 3\cdot10^7$ (solid curve 2) and 5.6% for $\mathrm{Re} = 3\cdot10^6$ (solid curve 3), whereas in the absence of viscosity at energy values corresponding to these maxima the increase in K is 17 and 10.5% (solid curve 1).

As the Mach number of the incident flow increases from $M_\infty = 0.75$ to $M_\infty = 0.8$, the share of the wave drag in the total drag of the airfoil increases from 83.7% in the variant for $\mathrm{Re} = 3\cdot10^7$ in Fig. 2a to 96.7% in the corresponding variant in Fig. 2b (solid curves 2) and from 76.6% in the variant for $\mathrm{Re} = 3\cdot10^6$ in Fig. 2a to 93% in the corresponding variant in Fig. 2b (solid curves 3). Naturally, this leads to the fact that in this case the relative values of the lift-drag ratio upon energy input with and without account for the viscosity become comparable: these values are 1.9% for $\mathrm{Re} = 3\cdot10^6$, 3% for $\mathrm{Re} = 3\cdot10^7$, and 2.8% and 3.5% at $\mathrm{Re} = \infty$, respectively. In the above variants of calculations with account for the viscosity, the displacement thickness did not exceed $8\cdot10^{-4}$ for $\mathrm{Re} = 3\cdot10^6$ and $4\cdot10^{-4}$ for $\mathrm{Re} = 3\cdot10^7$, which confirms the legitimacy of using the results of solving the energy input problem from the point of view of the nonviscous liquid–boundary layer model with subsequent recalculation of the aerodynamic characteristics.

A decrease in the airfoil thickness from $C = 12\%$ to $C = 8\%$ (Fig. 2b and Fig. 3a, respectively) leads to a considerable increase in the absolute value of the lift-drag ratio K with no change in the character of the dependence of K on the input energy. An increase in the Mach number of the incident flow leads to a sharp decrease in the fineness ratio of the airfoil. This is seen from a comparison of the results presented in Fig. 2a and b for an airfoil of thickness $C = 12\%$ over which air passes with $M_\infty = 0.75$ and 0.8, respectively, and from a comparison of the results in Fig. 3a and b for an airfoil of thickness $C = 8\%$ over which air passes with $M_\infty = 0.8$ and 0.85.

The appearance of a maximum in the dependence of the fineness ratio of the airfoil on the input energy with account for the viscosity is due to the nonmonotonic change in its drag (see Fig. 4).

The dashed lines in Figs. 2 and 3 correspond to the energy input zone $3.567 \le x \le 3.600$. With such a location of the zone the obtained effects (an increase in K and the existence of its maximum) are preserved qualitatively; however, the values of K therewith are somewhat smaller.

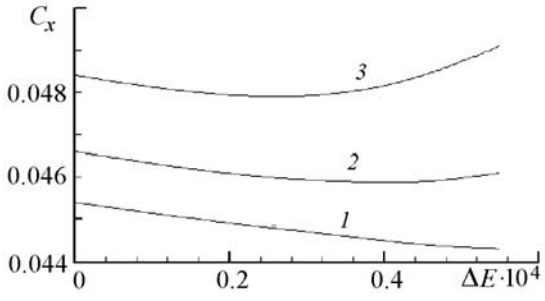

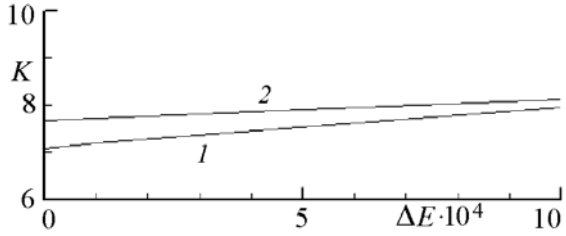

Fig. 4. Drag coefficient of the airfoil versus the input energy at $M_\infty = 0.8$ and $C = 12\%$ for various Reynolds numbers: 1) $Re = \infty$; 2) $3 \cdot 10^7$; 3) $3 \cdot 10^6$ (energy input zone $3.838 \le x \le 3.864$).

Fig. 5. Lift-drag ratio K of the airfoil versus the input energy ($M_\infty = 0.8$ and $C = 12\%$): 1) symmetrical airfoil section over which air passes at an angle of attack $\alpha = 3^o$; 2) asymmetrical airfoil section over which air passes at an angle of attack $\alpha = 0^o$.

Figure 5 shows the influence of the shape of the airfoil on its lift-drag ratio at one-way energy input (from below) (without taking into account the viscosity). Curve 1 corresponds to a symmetrical airfoil section over which air passes at an angle of attack $\alpha = 3^o$. Curve 2 corresponds to an asymmetrical airfoil section over which air passes at an angle of attack $\alpha = 0^o$ obtained as result of optimizing its shape in terms of the lift-drag ratio with a restriction on the minimum lifting force for the Mach number $M_\infty = 0.85$ (equal approximately to the lifting force of the symmetrical airfoil section at $\alpha = 3^o$ without energy input). The thickness ratio is the same: $C = 12\%$. In both cases, there is a monotonic increase in the lift-drag ratio with increasing energy input. In should be noted, however, that in the case of the symmetrical airfoil section the energy input leads to an increase in both the drag and the lifting force, and for the asymmetrical airfoil section the drag decreases with the lifting force remaining unaltered.

Conclusions. The investigation of the influence of pulsed-periodic energy input on the gas dynamics of the transonic flow of a symmetrical airfoil section with account for the real thermodynamic properties of the air has shown that account of these properties practically does not influence the wave drag of the airfoil, but leads to a considerable lowering of the temperature level as compared to the ideal gas model.

The investigation of the influence of viscosity on the aerodynamic characteristics of lifting airfoils in the boundary layer approximation at pulsed periodic energy input has shown that it is possible to increase the lift-drag ratio, though by a smaller value as compared to the nonviscous flow over the airfoil.

It has been established that an increase in the lift-drag ratio for a symmetrical airfoil section occurs with an increase in both the drag and the lifting force, and for an asymmetric airfoil section it occurs with a decrease in the drag and no change in the lifting force.

NOTATION

a, normalized velocity of sound; C, relative thickness of the airfoil section; C_d, viscous drag coefficient of the airfoil; C_x, total drag coefficient of the airfoil; $d\tau$, infinitely small element of the arc of the wing profile contour; e, energy density of the gas (energy of a unit volume); E, normalized specific energy; h, specific enthalpy; K, lift-drag ratio of the airfoil; M, local Mach number; M_∞, Mach number of the incident flow; p, normalized pressure; p_∞, windblast pressure, atm; Re, Reynolds number; Re_{tj}^{**}, Reynolds number of transition on the upstream and downstream faces of the airfoil, $j = 1, 2$; T, normalized temperature; T_m, normalized characteristic vibrational temperature, K; T_{vm}, characteristic vibrational temperature, K; T_∞, incident flow temperature, K; v_{end}, normalized velocity in the small neighborhood of the end point; v_{tj}, normalized velocity at the transition point on the upstream and downstream faces of the airfoil, $j = 1, 2$; v_τ, normalized velocity on the wing profile contour; v_∞, incident flow velocity, m/sec; x, normalized coordinate along the airfoil chord; x_m, molar fraction of the mth component of the air; α, angle of attack; γ, adiabatic index; δ^{**}, normalized momentum thickness; δ_k^{**}, normalized momentum thickness in the small neighborhood

of the end point; δ_j^{**}, normalized momentum thickness on the upstream and downstream faces of the airfoil, j = 1, 2; Δ_j, normalized extent of the turbulent boundary layer for the upstream and downstream contours, j = 1, 2; Δe, normalized energy input to a unit volume of the gas; ΔE, normalized total input energy in a period; ΔS, area of the energy input zone normalized to the squared length of the airfoil chord; Δt, normalized period of energy input; ε, normalized internal energy; ν, normalized kinematic viscosity coefficient; ρ, normalized density; ω, dimensionless energy input frequency. Subscripts: d, friction drag; j, airfoil face number; end, end point of the airfoil; m, air component number; t, turbulence; vm, vibrational temperature of the mth component; x, total drag; τ, tangent direction to the wing profile contour; ∞, incident flow; **, momentum thickness.

REFERENCES

1. P. Yu. Georgievsky, V. A. Levin, and O. G. Sutyrin, Instability of front separation regions initiated by upstream energy deposition, *Int. Conf. on Methods of Aerophys. Res.*, 30 June–6 July 2008, Novosibirsk, Abstracts. Pt. II, Publ. House "Parallel," Novosibirsk (2008), pp. 161–162.
2. A. A. Zheltovodov and E. A. Pimonov, Numerical research of supersonic flows features in conditions of localized energy deposition and verification of calculations, *Int. Conf. on Methods of Aerophys. Res.*, 5–10 February 2007, Novosibirsk, Proc. Pt. I, Publ. House "Parallel," Novosibirsk (2007), pp. 236–245.
3. S. M. Aul'chenko, V. P. Zamuraev, and A. P. Kalinina, Nonlinear effects of interaction of pulsed-periodic energy input and the shock-wave structure in the transonic flow over airfoil sections, *Pis'ma Zh. Tekh. Fiz.*, **32**, Issue 1, 6–11 (2006).
4. S. M. Aul'chenko, V. P. Zamuraev, and A. P. Kalinina, Influence of nonsymmetric pulsed-periodic energy input on the aerodynamic characteristics of airfoil sections, *Prikl. Mekh. Tekh. Fiz.*, **48**, No. 6, 70–76 (2007).
5. S. M. Aul'chenko, V. P. Zamuraev, and A. P. Kalinina, Aerodynamic characteristics of velocity profiles at energy input, *Prikl. Mekh. Tekh. Fiz.*, **50**, No. 5, 36–45 (2009).
6. M. A. Starodubtsev, Control of transonic flow over an airfoil by heat exchange, in: *Scientific Annals of the Central Aerohydrodynamic Institute*, **38**, No. 1/2, 36–40 (2007).
7. S. Raghunathan and D. Mitchell, Computed effects of heat transfer on the transonic flow over an aerofoil, *AIAA J.*, **33**, No. 11, 2120–2127 (1995).
8. A. V. Kazakov, M. N. Kogan, and V. A. Kuparev, Optimization of protracting of the laminar-turbulent transition by local heating of the surface, *Izv. Ross. Akad. Nauk*, *Mekh. Zhidk. Gaza*, No. 4, 90–99 (1995).
9. V. A. Levin, V. G. Gromov, and N. E. Afonina, Numerical investigation of the influence of local energy input on the aerodynamic resistance and heat transfer of spherical bluntness in a supersonic gas flow, *Prikl. Mekh. Tekh. Fiz.*, **41**, No. 5, 171–179 (2000).
10. A. N. Kraiko, Analytical representation of the thermodynamic functions of air, *Inzh. Zh.*, **4**, No. 3, 548–550 (1964).
11. G. Yu. Stepanov, *Hydrodynamics of the Blade Cascades of Turbomachines* [in Russian], Fizmatgiz, Moscow (1962).
12. A. M. Elizarov, N. B. Il'inskii, and A. V. Potashev, *Inverse Boundary-Value Problems of Aerohydrodynamics* [in Russian], Nauka, Moscow (1994).
13. S. M. Aul'chenko, A. F. Latypov, and Yu. V. Nikulichev, Experience in optimization of the aerodynamic characteristics of operating airfoil sections, *Prikl. Mekh. Tekh. Fiz.*, **43**, No. 1, 60–64 (2002).
14. *Table of Standard Atmosphere*. All-Union State Standard 4401-64, State Committee of Standards, Measures, and Measuring Devices of the USSR, Moscow (1964).